The theory of variances in equilibrium reconstruction

Leonid E. Zakharov,[1] Jerome Lewandowski,[1] Elizabeth L. Foley,[2] Fred M. Levinton,[2] Howard Y. Yuh,[2] Vladimir Drozdov,[3] and D. C. McDonald[3]
[1]*Princeton Plasma Physics Lab, Princeton University, Princeton, New Jersey 08543, USA*
[2]*Nova Photonics, Princeton, New Jersey 08540, USA*
[3]*Euratom/UKAEA Fusion Association, Culham Science Centre, Abingdon, Oxon, OX14 3DB, United Kingdom*

(Received 21 December 2007; accepted 11 August 2008; published online 4 September 2008)

The theory of variances of equilibrium reconstruction is presented. It complements existing practices with information regarding what kind of plasma characteristics can be reconstructed, how accurately, and what remains beyond the abilities of diagnostic systems. The σ-curves, introduced by the present theory, give a quantitative assessment of quality of effectiveness of diagnostic systems in constraining equilibrium reconstructions. The theory also suggests a method for aligning the accuracy of measurements of different physical nature and for improvements of numerical algorithms used in reconstruction. © *2008 American Institute of Physics*.
[DOI: 10.1063/1.2977480]

I. INTRODUCTION

The solution of the Grad–Shafranov (GSh) equation (Ref. 1)

$$\Delta^*\bar{\Psi} \equiv \frac{\partial^2\bar{\Psi}}{\partial r^2} - \frac{1}{r}\frac{\partial\bar{\Psi}}{\partial r} + \frac{\partial^2\bar{\Psi}}{\partial z^2} = -T - r^2P, \quad \bar{\Psi} \equiv \frac{\Psi}{2\pi}, \tag{1}$$

$$T = T(\bar{\Psi}) \equiv \bar{F}\frac{d\bar{F}}{d\bar{\Psi}}, \quad P = P(\bar{\Psi}) \equiv \frac{d\bar{p}}{d\bar{\Psi}},$$

$$\mathbf{B} = \mathbf{B}_{\mathrm{pol}} + \frac{1}{r}\bar{F}(\bar{\Psi})\mathbf{e}_\phi, \quad \mathbf{B}_{\mathrm{pol}} = \frac{1}{r}(\nabla\bar{\Psi}\times\mathbf{e}_\phi), \tag{2}$$

$$\bar{p} = \mu_0 p(\bar{\Psi}), \quad \bar{j} \equiv \mu_0 j_\phi = \frac{1}{r}T + rP$$

gives the most basic information on the magnetic configuration, which is necessary for all physics models of the tokamak plasma. Here, r,ϕ,z, are cylindrical coordinates reflecting axisymmetry of tokamak plasma, Ψ is the poloidal magnetic flux, B_ϕ is the toroidal magnetic field, p is the plasma pressure, and j_ϕ is the toroidal current density.

Equation (1) is two-dimensional, and its solution $\bar{\Psi}(r,z)$ is determined by the shape of the plasma boundary and by the two one-dimensional functions $T(\bar{\Psi}),P(\bar{\Psi})$ on the right-hand side (RHS) representing the current distribution inside the plasma. Correspondingly, the variances in the magnetic configurations are related to uncertainties in the plasma boundary and in two profiles $T(\bar{\Psi}),P(\bar{\Psi})$. The present paper gives the theory that allows the evaluation of these variances in equilibrium reconstruction.

Determination of the plasma boundary from external magnetic measurements can be considered as a separate problem, not directly related to the GSh equation. Its reconstruction is linked in a straightforward way with the accuracy of external magnetic measurements, which can be improved upon necessity. We have intentionally neglected (except for one example) the discussion of boundary reconstruction in order to focus on the more challenging problem of reconstruction of plasma profiles.

If the plasma boundary is reconstructed in some manner, the measured distribution of the magnetic field $\mathbf{B}_{\mathrm{pol}}$ along the plasma boundary restricts the choice of the two functions P,T in the right-hand side of the GSh equation. This effect, evident in equilibrium calculations of noncircular plasmas, motivated the first equilibrium reconstruction as early as 1973 (Ref. 2) in an attempt to recover the current density (and magnetic configuration) from information on the measured $\mathbf{B}_{\mathrm{pol}}$ outside the plasma. At present, reconstruction is a standard tool for interpreting the geometry of magnetic configurations due to the wide use of the EFIT code (Refs. 3 and 4) and its modifications.

Nevertheless, having only external measurements in tokamaks, the two unknown functions in the right-hand side of Eq. (1) can be reconstructed only in a limited way. Thus, in tokamaks with a circular cross section (in a high aspect ratio approximation) only integral parameters such as plasma current I_{pl}, internal inductance l_i, and Shafranov's β_j (Ref. 6) can be determined from external magnetic measurements (which include the diamagnetic loop). An outstanding example of a noncircular configuration with the same property of "hiddenness" was theoretically described by Bishop and Taylor in 1985 (Refs. 7 and 8). On the other hand, all equilibrium calculations show a distinctive effect of the current distribution on the external magnetic fields in noncircular plasmas, indicating that the shaping helps to retrieve more information about internal plasma profiles from external measurements.

But in any case, internal measurements are necessary. Because of the extreme importance of the equilibrium information, different diagnostics are being developed to provide additional information for reconstruction of the current distribution inside the plasma. Examples include kinetic measurements of electron and ion temperatures, plasma density, contribution of the fast particles to the plasma pressure, polarimetry, measuring the line integrated Faraday rotation of

polarized light from the laser beam,[9,10] or spectral lines,[11–13] signals related to motional Stark effect[14] (MSE), position of resonant surfaces from internal magnetohydrodynamic modes, etc.

Still, up to now, even with additional internal measurements the objective assessment (see, e.g., Ref. 15) of the value of equilibrium reconstruction has not been possible and the reconstruction itself remains a sort of "art" in numerical simulations rather than a science. One of the most advanced techniques, based on the accumulation of the data base of equilibria and singular value decomposition (SVD) analysis of it, was developed for the National Compact Stellarator project in Ref. 16.

In addition, it was noticed a long time ago (sometimes with confusing statements, e.g., Ref. 5) that although it is not possible to reconstruct the current density on the right-hand side of the GSh equation, the important integral parameters (β_j and l_i, introduced by Shafranov in the early 1960s as measurable ones) can be obtained with sufficient accuracy from the equilibrium reconstruction even for plasmas of noncircular cross section (see, e.g., Refs. 3 and 4).

Here, we describe a rigorous method, based on analysis of linear perturbations of equilibria, which allows assessment of uncertainties in equilibrium reconstruction, its overall value, and the contribution of measurements of different physical nature to the reconstruction. The same approach makes possible the quantitative evaluation of the quality of the diagnostic systems on existing and future machines. For practical use, the theory was implemented into ESC (Equilibrium and Stability Code) (Ref. 17), which is intrinsically based on linearization of the GSh equation as a method of its solution.

Section II describes the reduction of the problem of variances in equilibrium reconstruction to a matrix problem, which can be solved using the SVD technique (Ref. 18). Section III introduces the definition variances in equilibrium reconstruction and σ-curves. Section IV gives σ-curves for characteristic equilibrium configurations. Section V demonstrates the crucial role of internal measurements for reconstruction using the line polarization (MSE-LP) signals from the motional Stark effect as an example, relevant to the ITER diagnostics. Section VI outlines the possibility of aligning the accuracy levels of different measurements. Section VII addresses the issue of solving the nonlinear, ill-posed problem of reconstruction for the GSh equation. It gives a rigorous practical recipe, based on σ-curves, on how to perform the actual reconstruction in a stable and accurate manner. Section VIII outlines the possible applications of the theory of variances and its extension to other types of reconstructions of either one- or two-dimensional sources of signals.

II. THE FORMULATION OF THE PROBLEM OF VARIANCES

The theory of variances assumes that the reconstruction has been already performed and has generated a plasma shape and reconstructed functions $T(\bar{\Psi}), P(\bar{\Psi})$. The question to answer is what kind of other equilibria are possible within the given accuracy of diagnostics.

This problem is reduced to solving the linearized equilibrium problem

$$\bar{\Psi} = \bar{\Psi}_0(a) + \psi, \quad \Delta^*\psi + T'_{\bar{\Psi}}\psi + P'_{\bar{\Psi}}\psi = -\delta T(a) - \delta P(a) r^2 \tag{3}$$

for N possible perturbations of the plasma boundary ξ, and the functions T, P, δT, and δP, which can be represented as

$$\xi = \sum_{n=0}^{n<N_\xi} A_n \xi^n(\theta), \quad \delta T = \sum_{n=0}^{n<N_T} T_n f^n(a), \tag{4}$$

$$\delta P = \sum_{n=0}^{n<N_P} P_n f^n(a), \quad N = N_\xi + N_T + N_P,$$

$$\xi^n = \begin{cases} \cos m\theta, & \text{if } n = 2m \\ \sin m\theta, & \text{if } n = 2m+1 \end{cases}, \quad m = 0, 1, \ldots, \tag{5}$$

$$f^n = \cos\frac{\pi n a}{2},$$

where $0 \leqslant a \leqslant 1$ is the square root of the normalized toroidal flux, used throughout this paper as a flux coordinate, and θ is the poloidal angle on magnetic surface. The trigonometric basis functions $f^n(a)$ are used here as a particular choice for representing profile perturbations.

Instead of functions $T(\bar{\Psi})$, $P(\bar{\Psi})$ and their perturbations $\delta T(\bar{\Psi})$, $\delta P(\bar{\Psi})$, most of results in this paper are presented using an equivalent pair of current densities $\bar{j}_s(a)$, $\bar{j}_p(a)$ and their perturbations

$$\bar{j}(a,r) = \frac{R_0}{r}\bar{j}_s(a) + \left(\frac{r}{R_0} - \frac{R_0}{r}\right)\bar{j}_p(a), \tag{6}$$

$$\bar{j}_p(a) \equiv R_0 P, \quad \bar{j}_s(a) \equiv \frac{T}{R_0} + R_0 P,$$

where R_0 is the radius of the magnetic axis. Figure 1 shows an example of the background current density profiles $\bar{j}_s(a), \bar{j}_p(a)$ and the basis functions $f^n(a)$.

The displacement ξ, used here, specifies the plasma boundary perturbation $\delta r(\theta)$, $\delta z(\theta)$ in the following form:

$$r(a+\xi,\theta) = r(a,\theta) + r'_a\xi, \quad z(a+\xi,\theta) = z(a,\theta) + z'_a\xi, \tag{7}$$

$$\delta r(\theta) = r'_a(\theta)\,\xi|_{a=1}, \quad \delta z(\theta) = z'_a(\theta)\xi|_{a=1}.$$

The displacement ξ defined in this way is related to the solution of the linearized GSh equation (3),

$$\xi = -\left.\frac{\psi}{\bar{\Psi}'_0}\right|_{a=1}. \tag{8}$$

A numerical code, such as ESC (Ref. 17) can solve the linearized GSh equation (3) for each particular perturbation either of the plasma boundary or of the plasma profiles $\delta T, \delta P$. The signals on diagnostics for each of N solutions ψ can be calculated in a straightforward way. The linear relationship between the vector $\vec{X}$ of coefficients of perturbation

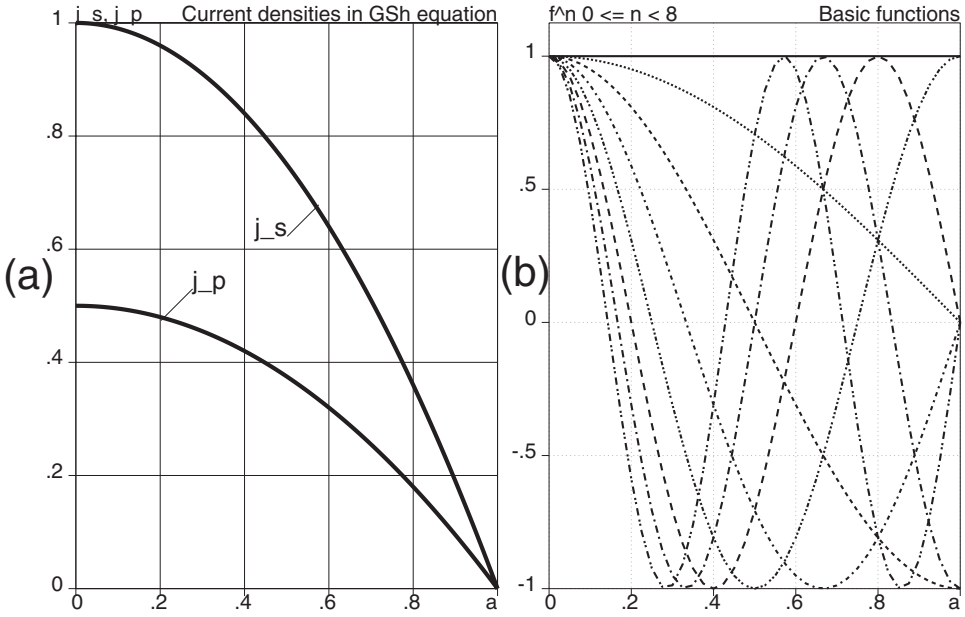

FIG. 1. (a) Background current density profiles $\bar{j}_s(a), \bar{j}_p(a)$, and (b) trigonometric expansion functions $f^n(a)$.

$$\vec{X} \equiv \{\underbrace{A_0, A_1, \ldots, A_{N_b-1}}_{N_\xi \text{ of } \xi}, \underbrace{T_0, \ldots, T_{N_T-1}}_{N_T \text{ of } \delta T}, \underbrace{P_0, \ldots, P_{N_P-1},}_{N_P \text{ of } \delta P}\} \tag{9}$$

and the vector $\delta\vec{S}$ of measured signals

$$\delta\vec{S} \equiv \{\underbrace{\delta\Psi_0, \ldots, \delta\Psi_{M_\Psi-1}}_{M_\Psi \text{ of } \delta\Psi}, \underbrace{\delta B_0, \ldots, \delta B_{M_B-1}}_{M_B \text{ of } \delta B_{\text{pol}}}, \underbrace{\delta S_0, \ldots, \delta S_{M_S-1}}_{M_S \text{ of others}}\} \tag{10}$$

can be written in matrix form,

$$\delta\vec{S} = \mathbf{A}\vec{X}, \quad \mathbf{A} = \mathbf{A}_{M\times N},$$
$$M \equiv M_\Psi + M_B + M_S, \quad N \equiv N_\xi + N_T + N_P. \tag{11}$$

Here, M_Ψ is the number of flux (saddle) loop signals, M_B is the number of signals from the local pickup coils, measuring poloidal magnetic field, M_S is the number of other signals (including the diamagnetic loop signal, MSE signals, and all other signals used for equilibrium reconstruction), while M is the total number of signals. Typically, $M > N$.

The response matrix $\mathbf{A}$, calculated for a representative set of perturbations for a given magnetic configuration, is the final product of equilibrium calculations in the theory of variances. After this step, the analysis of the matrix problem (11) is applicable to other reconstruction problems, reduced to inversion of the response matrix.

III. VARIANCES IN EQUILIBRIUM RECONSTRUCTION

After calculation of the response matrix $\mathbf{A}$, it is necessary to make a transition to a working matrix $\bar{\mathbf{A}}$, which weighs each signal δS_m in accordance with its accuracy ε_m (assumed to be known *a priori*),

$$(\bar{\mathbf{A}})_m^{0\le n<N} \equiv \frac{1}{\epsilon_m}(\mathbf{A})_m^{0\le n<N}, \quad \delta\bar{S}_m \equiv \frac{1}{\epsilon_m}\delta S_m, \quad \bar{\mathbf{A}}\vec{X} = \delta\bar{\vec{S}}. \tag{12}$$

Using the singular value decomposition (SVD) technique (Ref. 18), the matrix $\bar{\mathbf{A}}$ should be presented as a product of three matrices,

$$\bar{\mathbf{A}} = \mathbf{U}\cdot\mathbf{W}\cdot\mathbf{V}^T, \quad \mathbf{U} = \mathbf{U}_{M\times N}, \quad \mathbf{W} = \mathbf{W}_{N\times N}, \quad \mathbf{V} = \mathbf{V}_{N\times N}, \tag{13}$$

where $\mathbf{U}$ is a rectangular matrix with orthogonal columns, normalized to unity,

$$\mathbf{U}^T\cdot\mathbf{U} = \mathbf{I}, \quad I_i^k = \delta_i^k, \tag{14}$$

$\mathbf{I}$ is the identity matrix, $\mathbf{W}$ is a diagonal matrix containing the eigenvalues w^k of the problem

$$W_i^k = w^k\delta_i^k, \tag{15}$$

and the columns of $\mathbf{V}$ contain the normalized eigenvectors of the problem

$$\mathbf{V}^T\cdot\mathbf{V} = \mathbf{I}, \tag{16}$$

as it is described in Ref. 18. The expansion (13) is always possible and unique given the matrix $\bar{\mathbf{A}}$.

Each eigenvalue, determined by this procedure, is associated with an eigenvector $\vec{X}^k$ of coefficients (9), defined in terms of columns of the matrix $\mathbf{V}$ as

$$\vec{X}^k \equiv \gamma^k\mathbf{V}^k. \tag{17}$$

The factors γ^k scale each physical perturbation to the characteristic value of plasma perturbation $\xi_{\max} \simeq 1$, or the current densities $\bar{j}_{s,\max}, \bar{j}_{p,\max}$ (whatever is the most limiting one).

Calculation of standard deviations [or root mean square (RMS)] of the signals $\delta\vec{\bar{S}}^k$ generated by each eigenperturbation $\vec{X}^k$,

$$\delta\vec{\bar{S}}^k = \bar{\mathbf{A}}\vec{X}^k = \gamma^k w^k \vec{U}^k, \quad \sqrt{\frac{1}{M}\sum_{m=0}^{m<M}(\delta\bar{S}_m^k)^2} = \frac{\gamma^k w^k}{\sqrt{M}}, \tag{18}$$

allows the introduction of variances $\bar{\sigma}^k$ in reconstruction of each eigenperturbation as

$$\bar{\sigma}^k \equiv \frac{\sqrt{M}}{\gamma^k w^k}. \tag{19}$$

Variances $\bar{\sigma}^k$ in Eq. (19) specify uncertainties in the reconstruction of the plasma boundary ξ^k and current density $\delta T^k, \delta P^k$ for each eigenperturbation in an explicit form, i.e.,

$$\vec{X}^k \equiv \{\underbrace{A_0^k, A_1^k, \ldots, A_{N_b-1}^k}_{N_\xi \text{ of } \xi}, \underbrace{T_0^k, \ldots, T_{N_T-1}^k}_{N_T \text{ of } \delta T}, \underbrace{P_0^k, \ldots, P_{N_P-1}^k}_{N_P \text{ of } \delta P}, \}, \tag{20}$$

$$\xi^k = \bar{\sigma}^k \sum_{n=0}^{n<N_\xi} A_n^k \xi^n(\theta), \quad \delta T^k = \bar{\sigma}^k \sum_{n=0}^{n<N_T} T_n^k f^n(a),$$
$$\delta P^k = \bar{\sigma}^k \sum_{n=0}^{n<N_P} P_n^k f^n(a). \tag{21}$$

The amplitude of the uncertainties is proportional to the variances $\bar{\sigma}^k$. Because of the normalization of the matrix equation (12), the characteristic value of $\bar{\sigma}^k=1$ corresponds to a perturbation of the plasma boundary and current density in a magnetic configuration which is comparable to their background values, and still marginally visible by the diagnostics. The importance of variances $\bar{\sigma}^k$ is related to the following statement.

Perturbations $\vec{X}^k$ *with* $\bar{\sigma}^k > 1$, $(\log_{10}\bar{\sigma}^k > 0)$ *are essentially invisible to diagnostics with a given level of accuracy. The number of variances* $\bar{\sigma}^k < 1$ *in the spectrum of* $\bar{\sigma}^k$, *defined by Eq. (19), serves as a quantitative measure of quality of diagnostic systems for equilibrium reconstruction.*

In this paper, the perturbations with (a) $\bar{\sigma}^k < 0.1, \log_{10}\bar{\sigma}^k < -1$ are qualified as "well detectable," with (b) $0.1 \leqslant \bar{\sigma}^k < 1, -1 \leqslant \log_{10}\bar{\sigma}^k < 0$ called "barely visible," and (c) with $1 \leqslant \bar{\sigma}^k, 0 \leqslant \log_{10}\bar{\sigma}^k$ called "invisible."

The distinction between these three kinds of perturbations becomes obvious with the use of σ-curves, which are plots of $\log_{10}\bar{\sigma}^k$ as a function of k (assuming ascending ordering in σ^k). The intersection of the σ-curves with the zero level separates visible perturbations from those which cannot be reconstructed with a particular diagnostic system.

Based on an explicit solution $\bar{\Psi}_0 + \psi^k$ of the linearized equilibrium equation for each eigenperturbation, it is possible to calculate uncertainties in reconstruction of any physical quantity or plasma profile related to equilibrium. It is practically impossible to achieve good reconstruction of the current density profile, which would provide a full information on equilibrium. At the same time, such important profiles as q- and p-profiles can be reconstructed much better. Accordingly, it is possible to introduce variances $\bar{\sigma}_q^k, \bar{\sigma}_p^k$ for q- and p-profiles,

$$\bar{\sigma}_q^k \equiv \sqrt{\int_0^1 (\delta q^k)^2 da}, \quad \bar{\sigma}_p^k \equiv \sqrt{\int_0^1 \left(\frac{\delta p^k}{p_{\text{norm}}}\right)^2 da}, \tag{22}$$

all related to basic variances $\bar{\sigma}^k$ [Eq. (19)]. In Eq. (22), p_{norm} is the normalization value of plasma pressure, suggested here as

$$p_{\text{norm},MPa} \equiv \frac{I_{MA}^2}{20 S_{m^2}}. \tag{23}$$

This value corresponds to the average plasma pressure with $\beta_j = 1$ in Shafranov's definition

$$\beta_j = \frac{20\int p_{MPa} dS_{m^2}}{I_{\text{pl},MA}^2}, \tag{24}$$

where I_{MA} is the plasma current, and S_{m^2} is the plasma poloidal cross section.

The variances in integrated profiles (such as q- and p-profiles) are typically smaller than $\bar{\sigma}^k$, and these profiles can be reconstructed with a better certainty than, e.g., the current density. In the situation when q- and p-profiles cannot be reconstructed it is still possible to expect that, at least, such important quantities as plasma thermal W_{th} and magnetic W_{pol} energies can be reconstructed with a reasonable accuracy. In a dimensional form they can be replaced by parameters β_j^V and l_i defined by the following relationships:

$$W_{\text{th},MJ} \equiv \frac{3}{2}\int p dV, \quad \beta_j^V \equiv \frac{\frac{2}{3}W_{\text{th},MJ}}{0.1\pi R_{\text{ext},m} I_{\text{pl},MA}^2},$$
$$W_{\text{pol},MJ} = \frac{1}{2\mu_0}\int B_{\text{pol}}^2 dV, \quad l_i \equiv \frac{W_{\text{pol},MJ}}{0.1\pi R_{\text{ext},m} I_{\text{pl},MA}^2}, \tag{25}$$

where $R_{\text{ext},m}$ is a reference major radius of the plasma. The associated $\bar{\sigma}_{\beta_j^V}^k$ and $\bar{\sigma}_{l_i}^k$ are defined as

$$\bar{\sigma}_{\beta_j^V}^k \equiv \delta(\beta_j^V)^k, \quad \bar{\sigma}_{l_i}^k \equiv \delta l_i^k, \tag{26}$$

where variances $\delta(\beta_j^V)^k$ and δl_i^k are associated with a particular eigenvector $\vec{X}^k$ of perturbations.

The next section gives examples of σ-curves for some equilibrium configurations.

IV. SIGMA-CURVES FOR RECONSTRUCTION BASED ON MAGNETIC MEASUREMENTS

The ESC code[17] has been slightly modified in order to calculate w_k and variances in the current density, q-, p-profiles, and in β_j^V and l_i for different kinds of tokamak equilibria. They are presented in the order of complexity. In all examples the expansion functions $f^n(a)$ are taken in the trigonometric form (5) illustrated in Fig. 1(b).

For examples of this section, which rely only on magnetic field information, it was assumed that the poloidal mag-

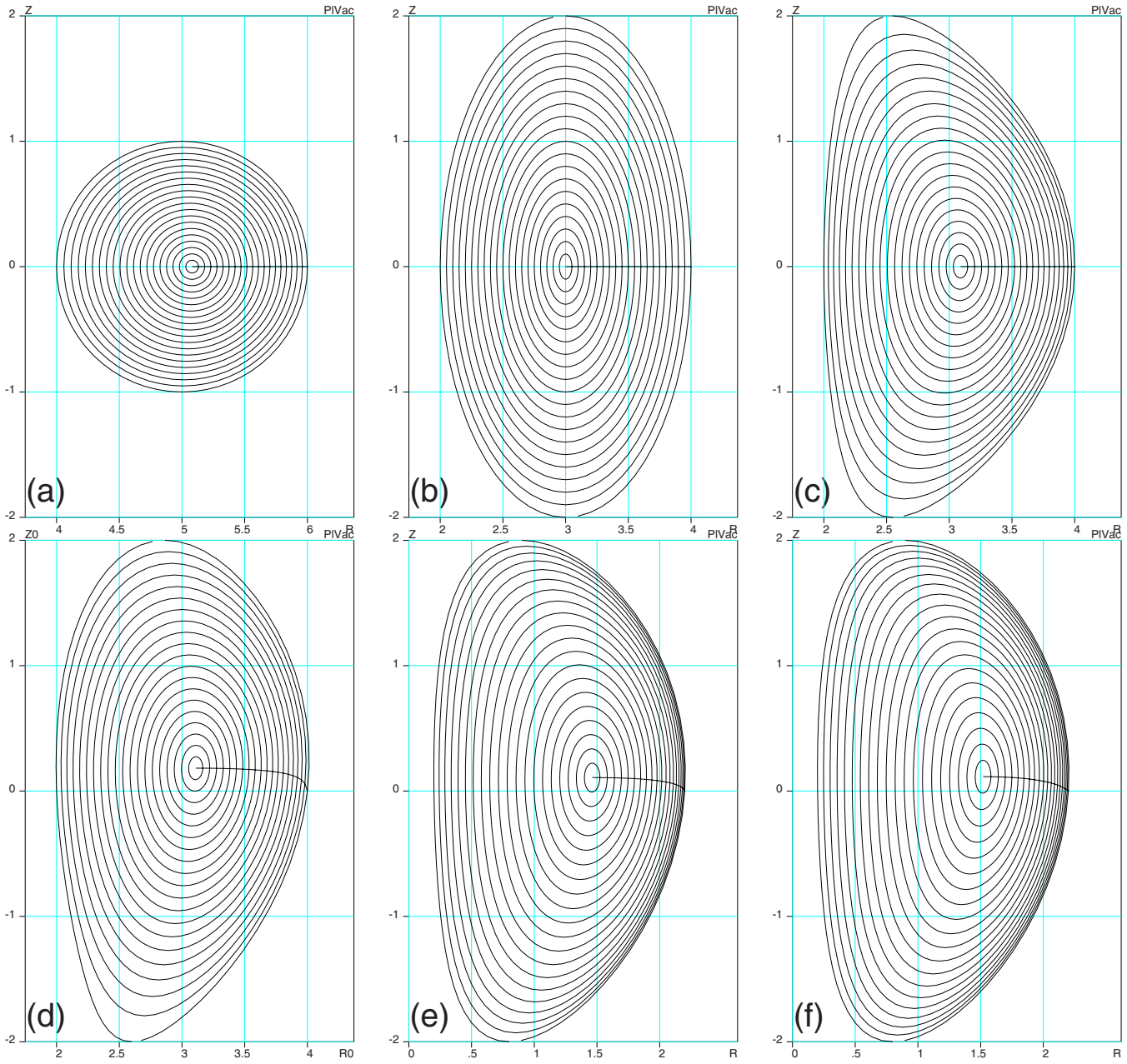

FIG. 2. (Color online) (a) Large aspect ratio $R/a=5$ equilibrium with a circular cross section. (b) Equilibrium with an elliptic cross section (elongation 2 and aspect ratio $R/a=3$). (c) D-shaped up-down symmetric equilibrium (elongation 2, $R/a=3$). (d) D-shaped up-down asymmetric equilibrium (elongation 2, $R/a=3$). (e) Low aspect ratio equilibrium (elongation 2, $R/a=1.25$) with $\beta=0.13$. (f) Low aspect ratio equilibrium (elongation 2, $R/a=1.25$) with $\beta=0.31$.

netic field $B_{\mathrm{pol}}(\theta)$ was "measured" at 64 equidistant positions at the plasma surface with absolute accuracy of 1% of its average value, the poloidal magnetic flux $\delta\Psi(\theta)$ is measured with the accuracy of 1% of its value inside the plasma, and the accuracy of the diamagnetic signal $\Delta\Phi$ is 0.1% of the toroidal magnetic flux Φ inside the plasma. In addition, the relative accuracy of 1% was introduced into uncertainties of the signals. Figure 2 shows four equilibrium configurations with circular [Fig. 2(a)], elliptic [Fig. 2(b)], and D-shaped [Figs. 2(c) and 2(d)] cross sections as well as two configurations for spherical tokamaks with a moderate [Fig. 2(e)] and a high [Fig. 2(f)] beta. In all configurations the safety factor at the magnetic axis is close to unity, $q_0 \simeq 1$.

The sigma curves, i.e., $\log_{10} \bar{\sigma}^k$ as functions of the eigenvalue number k, for these six cases are shown in Fig. 3. In all examples in Fig. 3 it is assumed that the plasma shape is already known, $\delta\Psi(\theta)=0$ (fixed boundary case), and the problem is in reconstruction of the plasma interior. The effect of the unknown plasma boundary is illustrated separately.

The solid curve in each frame represents the basic σ-curve for reconstruction of the right-hand side of the GSh equation (1). This σ-curve determines the quality of reconstruction of magnetic configuration.

Two σ-curves labeled "p" and "q" represent $\log_{10} \sigma_p$ and $\log_{10} \sigma_q$ as functions of k as defined by Eq. (22). In addition, two σ-curves labeled "β^V" and "li" for integral parameters β_j^V and l_i, defined by Eq. (25), are shown in each case. These two curves are important for assessment of quality of recon-

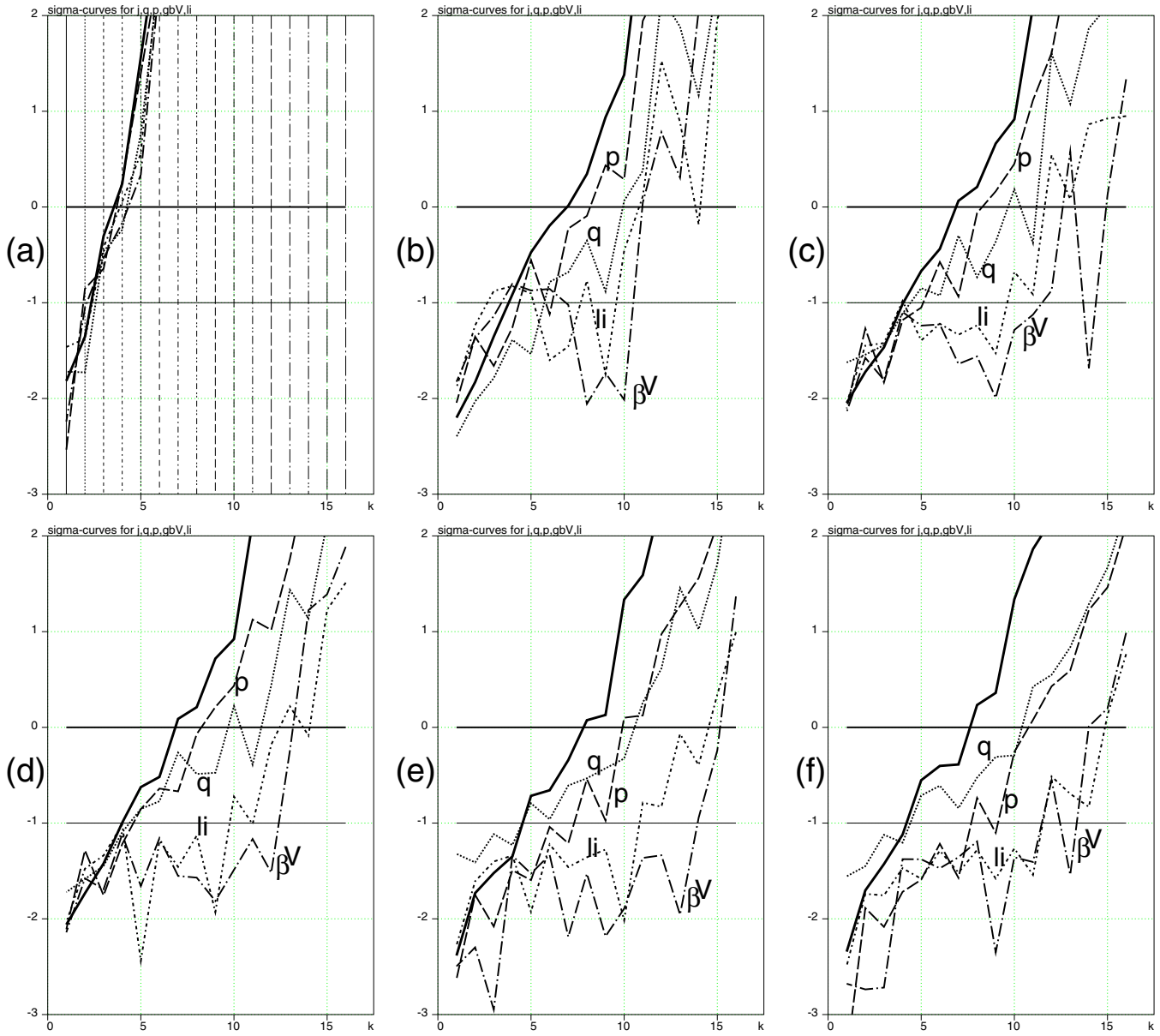

FIG. 3. (Color online) Numerically calculated σ-curves for six equilibria of Fig. 2 with known plasma boundaries: $\log_{10}\bar{\sigma}^k$ (solid lines) is variance in reconstruction of the right-hand side of the GSh equation, $\log_{10}\bar{\sigma}_p^k$ ("p"-labeled long-dashed lines) is the variance in p-profile, $\log_{10}\bar{\sigma}_p^k$ ("q"-labeled dashed lines) is the variance in q-profile, $\log_{10}\bar{\sigma}_{\beta_j^V}^k$ ("β^V"-labeled dashed-dotted lines) is the variance in β_j^V, and $\log_{10}\bar{\sigma}_{l_i}^k$ ("li"-labeled short-dashed-dotted lines) is the variance in l_i. The type of vertical lines in frame (a) is linked to the index k of eigenperturbations. These types of lines are used later on for plots specific for each eigenperturbation (e.g., Fig. 6).

struction of plasma thermal and magnetic energies.

Two horizontal lines separate "invisible" eigenperturbations ($\log_{10}\sigma>0$) from "barely visible" ($-1<\log_{10}\sigma<0$) and "well detectable"($\log_{10}\sigma<-1$).

As expected, the circular cross section [Fig. 3(a)] represents the worse case for reconstruction based on magnetic measurement. Only three eigenvectors of variances fell into categories of "well detectable" or "barely visible." All other eigenvectors cannot be reconstructed based on magnetic data.

It seems to be surprising from σ-curves in Fig. 3(a) that, in contradiction with the classical Shafranov theory, even β_j^V and l_i appear to be impossible to reconstruct. The reason for this paradox is that the σ-curves are calculated assuming that the signals of eigenperturbations fit the accuracy of measurements. Because of this normalization, the resulting amplitude of eigenperturbations can exceed the background level of the current density, as happens for all "invisible" eigenperturbations (with $\log_{10}\sigma^k>0$). At the same time, any additional information (even imprecise), which can limit the amplitude of the current density variances will resolve the paradox. In the present technique of variances such information can be introduced in a formalized way simply as another "signal."

Shaping of the plasma boundary makes equilibrium reconstruction based on magnetic measurements much more certain. In all shaped cases in Fig. 3 the reconstruction of six eigenperturbations in the RHS of the GSh equation is possible. The p- and q-profiles are reconstructed better than the

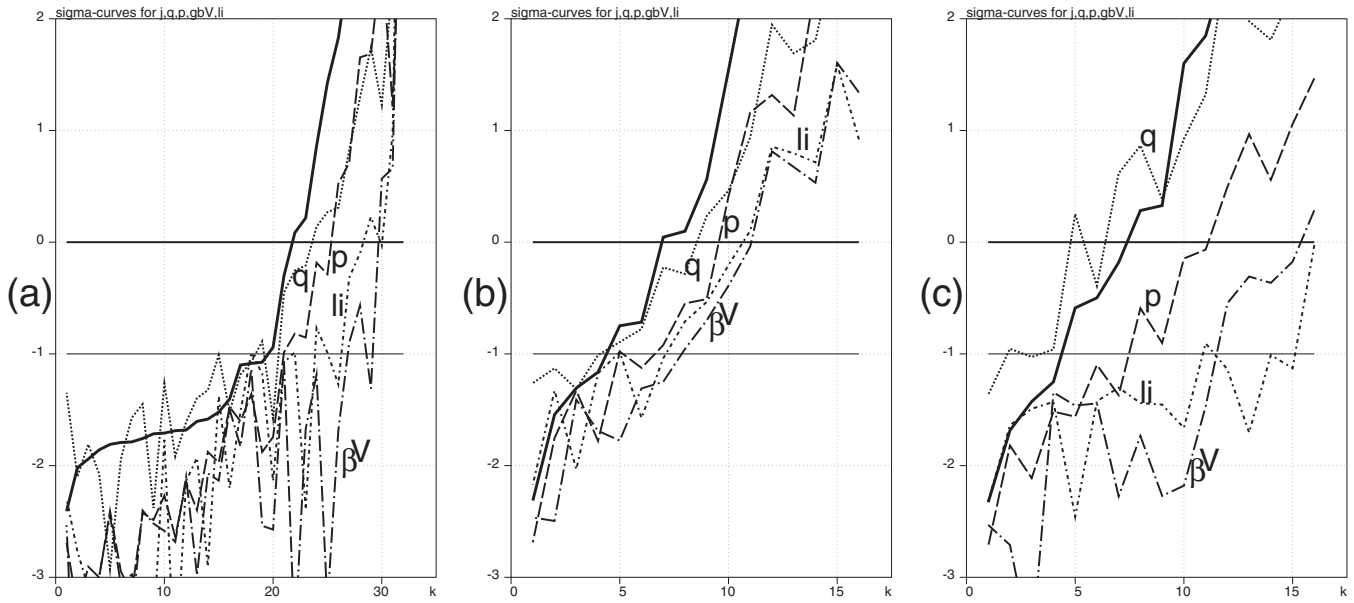

FIG. 4. Effect of free boundary, diamagnetic signal, and q-profile on reconstruction of the spherical tokamak case [see Fig. 3(e)] with a moderate β=0.13. (a) Sigma-curves in the case of free plasma boundary and enhanced range of eigenvalues. (b) Sigma-curves for the case of the absence of the diamagnetic signal. (c) The equilibrium with a nonmonotonic q-profile (q_0=4.5, $q_{\min} \simeq 2$, q_{edge}=13). The labels on the curves are the same as in Fig. 3.

RHS. For spherical tokamaks [Figs. 3(e) and 3(f)] the β_j^V parameter and corresponding thermal energy of the plasma can be well (better than 10%) reconstructed for a wide range of the eigenperturbations. The last two frames also illustrate the fact that the σ-curves are not sensitive to equilibrium reconstructed. They are much more sensitive to the diagnostics used.

Figure 4(a) illustrates the effect of free boundary on reconstruction of the spherical tokamak equilibrium in Fig. 3(e). In this case it is assumed that $\delta\Psi(\theta)$ is known in 16 points around the plasma with the accuracy of 1% of poloidal flux inside the plasma. Accordingly 16 perturbations of the plasma boundary have been included in the variances of the equilibrium. The major effect of the "free" boundary is the extension of the "visible" part of the spectrum of eigenvalues, which is almost horizontal on the basic σ-curve for the RHS of the GSh equation. This behavior is expected, because the reconstruction of the plasma boundary is essentially determined by the accuracy of external measurements. The improvement in accuracy shifts all σ-curves vertically, thus allowing improvements in plasma boundary reconstruction. On the other hand, the steep part of the σ-curves, which is related to reconstruction of the internal profiles, cannot be affected significantly by improvement of the accuracy of signals. Instead, for better reconstruction of internal profiles some additional information or internal diagnostics is necessary.

Because the effect of a "free" boundary, although important in practice, is straightforward, for the purposes of this paper it was dropped from consideration.

Figure 4(b) gives the σ-curves for the same case as in Fig. 3(e), but when the diamagnetic signal was excluded from consideration. The significant deterioration of the reconstruction of β_j^V and l_i is rather obvious from the behavior of the σ-curves, which confirms the importance of the diamagnetic signal for equilibrium reconstruction.

The effect of the nonmonotonic q-profile is illustrated in Fig. 4(c), which shows rather significant increase in variances of the q-profile.

V. POSSIBILITY OF COMPLETE RECONSTRUCTION WITH INTERNAL MEASUREMENTS

This section illustrates the crucial effect of internal measurements on equilibrium reconstruction. As an example, the ITER configuration (Fig. 5) with the plasma current I_{pl}=15 MA is considered.

The external magnetic diagnostics is assumed to be the same as described earlier. In addition, it is assumed that the internal line polarization signals of the motional Stark effect (MSE-LP) provide the pitch angle values $\arctan(B_z/B_{\text{tor}})$ (the ratio of the vertical and toroidal magnetic fields) in 21 pickup points. The relative and absolute accuracies are 1% and 0.1°, correspondingly.

Figure 6 provides the comparison of σ-curves and variances in p- and q-profiles with and without MSE-LP measurements.

With no internal measurements, not more than seven eigenperturbations in the RHS of the GSh equation can be considered detectable. The parameter β_j^V is reconstructed pretty well in the extended spectrum of perturbations $k \leqslant 13$. The q- and pressure p-profiles can be reconstructed well for only six eigenperturbations.

The additional information on the plasma profiles makes a crucial impact on reliability of equilibrium reconstruction, as is seen from Figs. 6(d)–6(f). Thus, two integral parameters β_j^V and l_i are not sensitive to the entire range $k \leqslant 16$ of per-

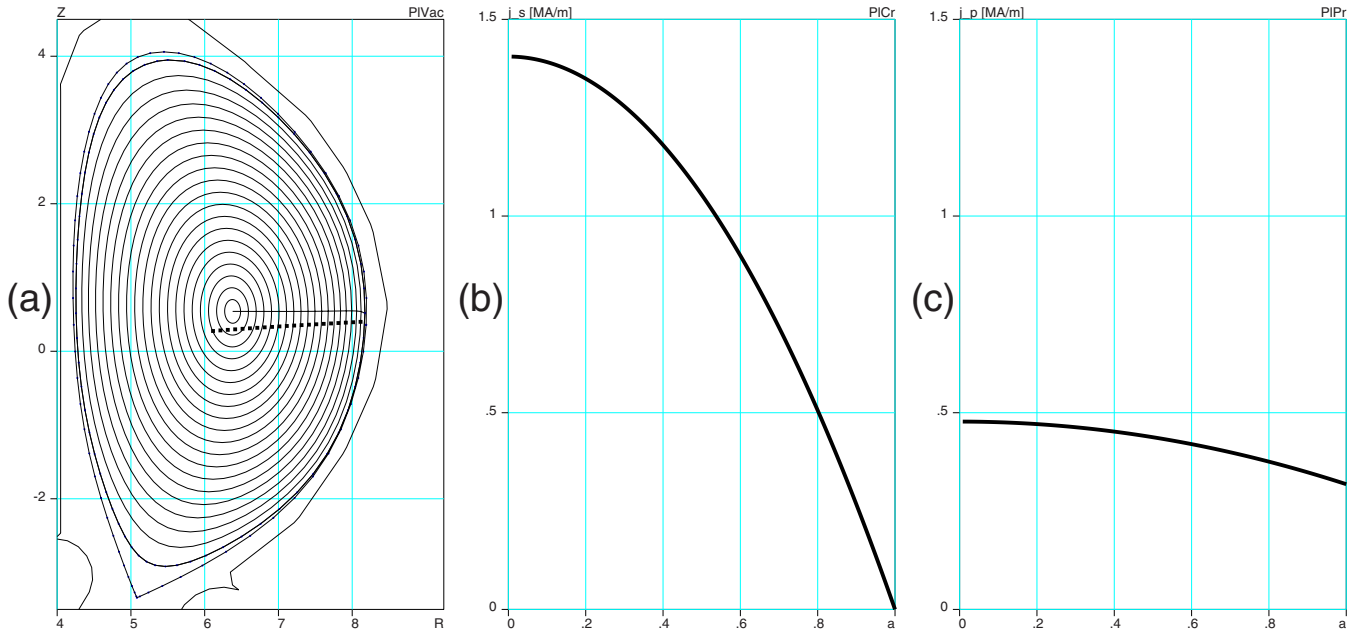

FIG. 5. (Color online) (a) Cross section of the ITER magnetic surfaces. Black dots point out the 21 MSE-LP pick-up points. (b) j_s-profile and (c) j_p-profile, which are used in equilibrium calculations.

turbations. In addition, both p- and q-profiles can be well reconstructed essentially in the twice larger range of eigenperturbations ($k \leqslant 15$) than without MSE-LP measurements.

For the case of ITER, the line shift signals from the motional Stark effect (MSE-LS) have been proposed in Ref. 19. The analysis of variances for this case was performed in Ref. 20. It has confirmed that also in the case of MSE-LS, the internal measurements of plasma profiles have a profound effect on reduction of variances.

VI. ALIGNMENT OF SENSITIVITIES OF SENSORS

The presented theory of variances allows the use of signals of different physical nature in the process of reconstruction. Even the transport calculations, which restrict the range of plasma profiles, can be included in the reconstruction as additional signals. The normalization of the working matrix using the sensitivity value of every signal takes into account the contributions of signals independently of the nature of the signal.

At the same time, the contribution of different signals into reconstruction is different. It is important that the presented theory of variances provides the way of an objective assessment of the role of each signal in the reconstruction. This is illustrated here using the example of the combination of MSE-LP and magnetic measurements.

Figures 7(a) and 7(c) show the normalized signals calculated from eight eigenperturbations. As it was pointed out, that eigenvalues (σ-curves) are normalized in a way that the signals from variances is within the error bars of measurements (in the RMS sense). The first 64 signals on these figures, represent the poloidal magnetic field measurements, while the last 21 ones are the MSE-LP signals from eigenperturbations.

It is evident that the load on MSE-LP and B_{pol} diagnostics is not uniform. The MSE-LP measurements make larger contribution to the reconstruction. Because of this, there is room for optimization of the entire diagnostic system. For example, the accuracy of MSE-LP measurements can be reduced, while the accuracy of B_{pol} measurements should be enhanced.

The general recipe for the optimal use of diagnostics of different physical nature is to align the sensitivity of sensors in such a way that the signals $\delta\bar{S}_m^k$ from eigenperturbations fill up the band $|\delta\bar{S}_m^k| \leqslant 1$ uniformly.

As an example, Figs. 7(b) and 7(c) show σ-curves and signals for the same set of measurements, but twice better accuracy in B_{pol} measurements and four times worse accuracy of MSE-LP signals. Because of better balance of the accuracy of the diagnostic, the resulting σ-curves are essentially the same, despite the significant reduction of requirements to the MSE diagnostics.

VII. USE OF σ-CURVES FOR OPTIMAL RECONSTRUCTION

Besides the assessment of the final reconstruction, the σ-curves can provide information for optimal organization of the iterative solving of the GSh equation in the process of fitting its solution and the current distribution to the measurements.

The problem is in making a compromise between the goal of the most accurate reconstruction and stability of iterations. The σ-curves can be calculated at every iteration, and then the current distribution could be composed from the eigenperturbations, whose k-spectrum is limited by the condition of elimination of "invisible" perturbations

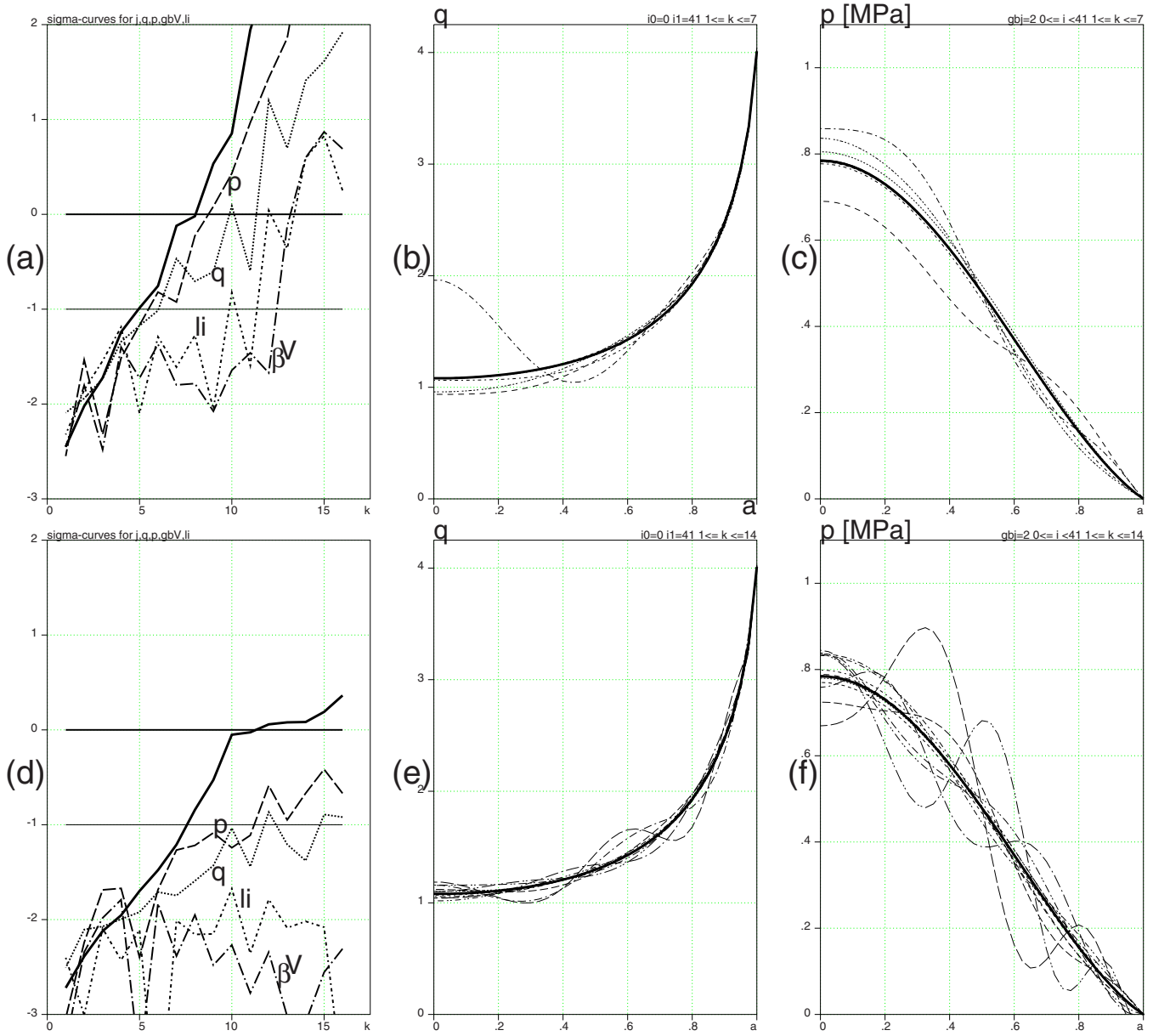

FIG. 6. (Color online) Variances in reconstruction of the ITER equilibrium example assuming a fixed plasma boundary. (a) σ-curves for reconstruction based on magnetic measurements. (b) Variances in q-profile corresponding to the first seven eigenperturbations. (c) Corresponding seven variances in the p-profile. The correspondence of the type of the curves to the index of eigenperturbations k is specified in Fig. 3(a) plasma. (d) σ-curves for reconstruction based on magnetic and MSE-LP measurements. (e) Variances in q-profile corresponding to the first 15 (!) eigenperturbations. (f) Variances in the p-profile for the first 15 eigenperturbations.

$$\log_{10} \bar{\sigma}^k < -r, \tag{27}$$

where the constant r is in the range $0.5 < r < 1$. The left boundary here should be determined experimentally from the marginal stability of iterations.

In this way, reconstruction with a poor set of signals, e.g., containing only external measurements, would be performed with a small set of free parameters leading to large variances and a reconstruction of limited value (which still could be very useful, e.g., for assessing the thermal energy ofplasma). On the other hand, in the case of good diagnostics, the stability of reconstruction will be provided even for the most accurate reconstruction possible.

The practical implementation of this algorithm is left for future development.

VIII. CONCLUSIONS

Calculation of σ-curves for variances of physical quantities using the SVD technique solves the problem of evaluation of uncertainties left in equilibrium reconstruction. The associated technique can be implemented into existing equilibrium reconstruction codes in order to generate information on variances in different plasma characteristics remaining after equilibrium reconstruction has been performed. In this regard, the theory covers the plasma numerical parameters (like β, l_i), plasma profiles (e.g., p, q) or two-dimensional characteristics (e.g., the neutron sources) as soon as the effect of eigenperturbations can be calculated.

The capability of calculating variances, now developed, has essentially completed the theory of equilibrium recon-

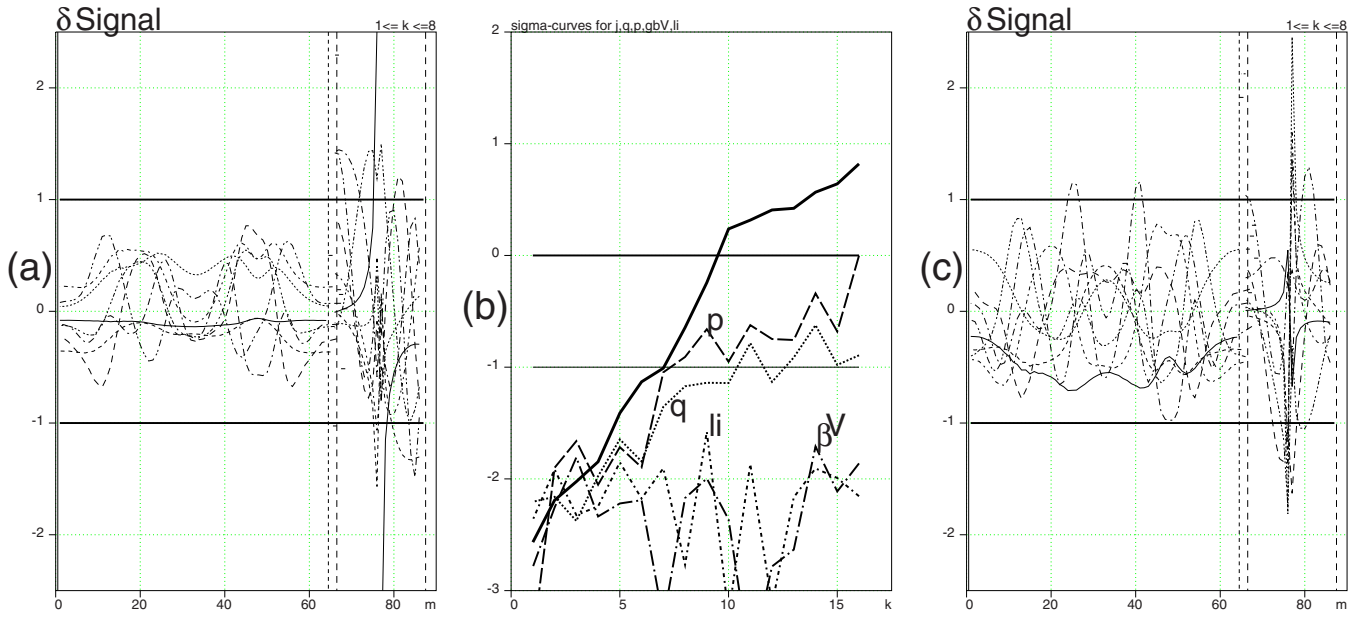

FIG. 7. (Color online) (a) Signals $\delta\bar{S}_m^k$ generated by eigenperturbations enumerated by k for the case of Figs. 6(d)–6(f). The horizontal axis represents the index "m" of the signal: $1 \leqslant m \leqslant 64$ corresponds to pickup coils of poloidal magnetic field, $m=65$ is the diamagnetic signal, $66 \leqslant m \leqslant 86$ represent the MSE-LP signals. The pointwise signals are connected by lines of different types in order to link them to the index of eigenperturbation [see Fig. 3(a)]. Two horizontal lines specify the range of normalized error bars. (b) σ-curves for fourfold reduced accuracy of MSE-LP measurements and twice enhanced accuracy of B_{pol} measurements. (c) Signals generated by eigenperturbations for the case (b).

struction. In particular, the quantitative evaluation of the quality of diagnostic systems on existing and future machines can be done based on the spectrum of "visible" perturbations and $\bar{\sigma}$-curves. The theory confirms that internal measurements of the magnetic field are crucial for reconstruction. In this regard, either MSE-LP (line polarization) or MSE-LS (line shift) signals from the plasma in addition to external measurements allow potentially for a complete reconstruction of both q- and p-profiles. The presented technique can be used to optimize the diagnostic set on any tokamaks. Contribution of any signal can be evaluated in a rigorous way and unambiguously.

This theory, which was illustrated here using a "traditional" set of signals, is, in fact, not limited to it. Any signal, pointwise or distributed (like Faraday rotation), as well as results of numerical simulations can be included as contributors into reconstruction.

In addition, the raw, rather than postprocessed, signals can be used in the reconstruction scheme based on this theory. This would take into account the "error propagation" effect in a formalized and self-consistent manner.

Implementation of the theory should be focused on realistic simulation of signals used in reconstructions and on developing working algorithms, based on σ-curves, for accurate and stable iterative solution of the GSh equation for reconstruction purposes.

ACKNOWLEDGMENTS

This work is supported by U.S. DOE Contract No. DE-AC020-76-CHO-3073. This work was also partly funded by the United Kingdom Engineering and Physical Sciences Research Council and by the European Communities under the contract of Association between EURATOM and UKAEA. The views and opinions expressed herein do not necessarily reflect those of the European Commission.

[1] V. D. Shafranov, Sov. Phys. JETP **6**, 545 (1958); Zh. Eksp. Teor. Fiz. **33**, 710 (1957); H. Grad and H. Rubin, in *Proceedings of the Second United Nations Conference on the Peaceful Uses of Atomic Energy* (United Nations, Geneva, 1958), Vol. 21, p. 190.
[2] A. V. Bortnikov, Yu. T. Baiborodov, N. N. Brevnov, L. E. Zakharov, V. G. Zhukovskii, D. V. Orlinskii, V. I. Pergament, M. K. Romanovskii, N. I. Sokolov, and Yu. M. Us, *Proceedings of Contributed Papers, Sixth European Conference on Plasma Physics and Controlled Fusion, Moscow, 1973* (European Physical Society, Plasma Physics Division, published by Joint Institute for Nuclear Research, Moscow, 1973), Vol. 1, p. 349.
[3] L. L. Lao, H. St. John, R. D. Stambaugh, A. G. Kellman, and W. Pfeiffer, Nucl. Fusion **25**, 1611 (1985).
[4] L. L. Lao, J. R. Ferron, R. J. Groebner, W. Howl, H. St. John, E. J. Strait, and T. S. Taylor, Nucl. Fusion **30**, 1035 (1990).
[5] J. P. Freidberg, M. Graf, A. Niemszewski, S. Schultz, and A. Shajii, Plasma Phys. Controlled Fusion **35**, 1641 (1993).
[6] L. E. Zakharov and V. D. Shafranov, *Reviews of Plasma Physics* (Consultants Bureau, New York, 1986), Vol. 11, p. 153.
[7] C. M. Bishop and J. B. Taylor, in *Proceedings of Contributed Papers, 12th European Conference on Controlled Fusion and Plasma Physics*, Budapest, 1985, edited by L. Pócs and A. Montvai (European Physical Society, Budapest, 1985), Vol. II, pp. 401–404.
[8] C. M. Bishop and J. B. Taylor, Phys. Fluids **29**, 1444 (1986).
[9] F. D. Marco and S. E. Segre, Plasma Phys. **14**, 245 (1972).
[10] H. Soltwisch, Rev. Sci. Instrum. **57**, 1939 (1986).
[11] W. P. West, D. M. Thomas, J. S. deGrassie, and S. B. Zheng, Phys. Rev. Lett. **58**, 2758 (1987).
[12] K. McCormick, F. X. Sîldner, D. Eckhartt, F. Leuterer, H. Murmann, H. Derfler, A. Eberhagen, O. Gehre, J. Gernhardt, G. v. Gierke, O. Gruber, M. Keilhacker, O. Klüber, K. Lackner, D. Meisel, V. Mertens, H. Röhr, K.-H. Schmitter, K.-H. Steuer, and F. Wagner, Phys. Rev. Lett. **58**, 491 (1987).
[13] D. Wröblewski, L. K. Huang, H. W. Moos, and P. E. Phillips, Phys. Rev. Lett. **61**, 1724 (1988).
[14] F. M. Levinton, R. J. Fonck, G. M. Gammel, R. Kaita, H. W. Kugel, E. T. Powell, and D. W. Roberts, Phys. Rev. Lett. **63**, 2060 (1989).
[15] V. D. Pustovitov, Nucl. Fusion **41**, 721 (2001).
[16] N. Pomphrey, E. Lazarus, M. Zarnstorff, A. Boozer, and A. Brooks, Phys. Plasmas **14**, p. 056103 (2007).

[17]L. E. Zakharov and A. Pletzer, Phys. Plasmas **6**, 4693 (1999).
[18]W. H. Press, S. A. Teukolsky, W. T. Vetterling, and B. P. Flannery, *Numerical Recipes in C* (Cambridge University Press, Cambridge, 1992), pp. 59–70.
[19]H. Y. Yuh, E. L. Foley, and F. M. Levinton, USIPO Report No. S006930-F, 2007.
[20]L. E. Zakharov, E. L. Foley, F. M. Levinton, and H. Y. Yuh, Plasma Phys. Rep. **34**, 173 (2008).